RSC Advances

ROYAL SOCIETY OF CHEMISTRY

www.rsc.org/advances

Overexpression of *div8* increases the production and diversity of divergolides in *Streptomyces* sp. W112†

Guishi Zhao,[a] Shanren Li,[a] Zhixing Guo,[a] Mingwei Sun,[a] and Chunhua Lu*[a]

a. *Key Laboratory of Chemical Biology (Ministry of Education), School of Pharmaceutical Sciences, Shandong University, Jinan, 250012, PR China. E-mail:ahua0966@sdu.edu.cn; Tel: 086-531-88382108*

† Electronic Supplementary Information (ESI) available: See DOI:

*Correspondence:

Chunhua Lu

Tel: +86-531-88382108, E-mail: ahua0966@sdu.edu.cn

Isolation and structure elucidation of divergolides from *Streptomyces* sp. HKI0576 revealed unusual ansamycin diversification reactions and the biosynthetic flexibility of the divergolide family. The production of divergolide E in *Streptomyces* sp. W112 was previously increased by overexpression of *div8*, which belongs to ATP-binding regulators of the LuxR family. In this study, we have further characterized the products of the *div8*-overexpressed mutant and five new divergolide congeners (**1**–**5**) were elucidated. Among them, **1**–**3** features conserved divergolide A skeleton, and **4** and **5** are lactone isomers and *seco* variant of divergolides E and D, respectively. Divergolides O–S (**1**–**5**) showed almost no toxicity to tested human cancer cell lines of MDA-MB-231, PC3 and HeLa at 50 μM. Whereas, **4** and **5** significantly inhibited the secretion of SPI-1 effectors.

Introduction

Ansamycins comprise a family of bioactive macrolactams, including the well-defined antitumor agents geldanamycins,[1] maytansinoids,[2] ansamitocins[3] and the antitubercular agents rifamycins.[4] Ansamycins are synthesized by type I polyketide synthase (PKS) analogy to macrolactones. The striking differences, however, are that the biosynthesis of ansamycins are started by loading 3-amino-5-hydroxybenzoic acid (AHBA) to the chain-initiation domain consisting of an acyl carrier protein (ACP) and an adenyltransferase, and terminated by releasing the nascent polyketide chains via intramolecular amidation.[5] Previously, we were approaching to novel ansamycins through PCR screening of AHBA synthase genes, which afforded twenty six AHBA synthase gene-positive strains from plant-associated and marine-derived actinomycetes.[6] Among these strains, *Streptomyces* sp. W112 isolated from the medicinal plant *Camptotheca acuminate* in Xiamen, China showed the potential of producing divergolides.[7] The divergolides A–D (Fig.S1), 19-membered naphthalenic ansamacrolactam antibiotics with antibacterial and antitumor activities, were first obtained from the endophytic *Streptomyces* sp. HKI0576 isolated from the stem of mangrove tree *Bruguiera gymnorrhiza*.[8, 9] Due to the low production yield, bioactive potential of divergolides was not able to be fully investigated. The divergolide biosynthetic gene cluster was elucidated by stable isotope labeling experiments[8] and genomic shotgun sequencing analysis[9]. To shed light on the exact mechanism of divergolide assembly, diversity of metabolites were detected by HPLC–HRMS from 200 L fermentation of *S.* sp. HKI0576 and divergoliges E–N (Fig.S1) were further purified. Our recently results suggested that the LAL regulator *div8* acts as an activator;[10] Constitutive overexpression of *div8* gene in strain W112 increased the products of divergolide E and produced new divergolide analogs.

We report herein the isolation and bioactivity of the five new divergolide derivatives, namely divergolides O-S (**1**–**5**) (Fig.1), from metabolites of the mutant strain W112OE*div8*.

Results and discussion

Solid-state fermentation (40 L) of the mutant strain W112OE*div8* was performed with ISP3 agar medium for 14 d at 28°C. The agar culture was extracted successively with EtOAc-MeOH (80 : 15), *v*/*v*). After removal of the solvents, the crude extract was isolated by repeated column chromatography (over RP_{18} silica gel, normal phase silica gel, Sephadex LH-20 and

semi-preparative HPLC). The pure divergolides O–S (**1**–**5**) (Fig. 1) were finally obtained by reversed-phase HPLC.

HRESIMS data indicated that divergolides O and P (**1** and **2)** have the same molecular

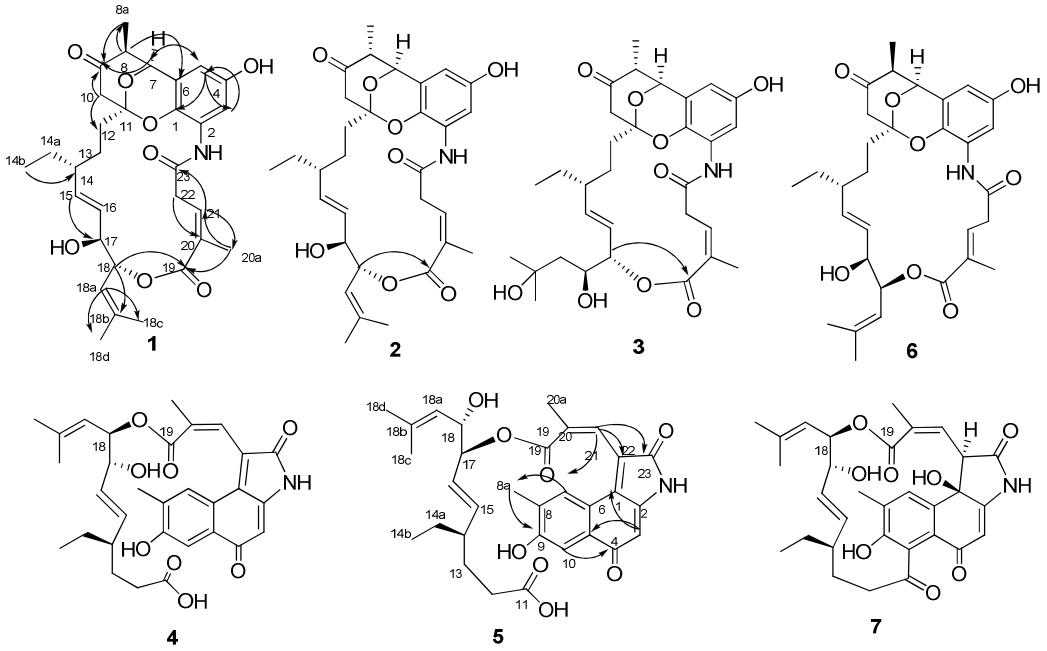

Fig. 1 Structures of divergolides O-S (**1** - **5**) and divergolides H(**6**) and E(**7**)

formula of $C_{31}H_{39}NO_8$ as that of divergolide H (**6**). Both ^{1}H NMR and ^{13}C NMR data (Table 1) of **1** and **2** exhibited strong similarities to those of the previously described divergolide H (**6**)[9]. The architecture of the overall *ansa* bridge was deduced from the NMR data, and further confirmed by the HMQC and HMBC correlations. A careful comparison of NMR data revealed some variations at position C-7, C-8a, C-20a. For **1** and **6**, the H-7 signals appeared as doublets, whereas in **2** singlet was observed. As a result, H-7 and H-8 show a *syn* orientation in **1** and **6**, but an *anti*-orientation in **2**. In **1** and **2**, a relatively downfield chemical shift for C-20a (δ_C = 20.7 ppm) indicated a C-20a *Z* configuration, in contrast with a C-20a *E* configuration in **6**, revealed by the relatively upfield chemical shift of C-20a (δ_C = 13.1 ppm). Moreover, for **1** and **2**, HMBC correlations between H-18 and C-19 confirmed the location of the ester moiety, which is the same as in **6**. The structure of divergolide A has been unambiguous determined based on the crystal structure[8], and divergolide H (**6**) also has been elucidated by comparison with those of A and further CD spectrum.[9]

The configuration of C-8a makes the difference between **1** and **2** was determined by the NOESY spectrum and the chemical shift of C-8a (δ_C 10.0, δ_H 1.03 in **1** and δ_C 15.0, δ_H 1.35 in **2**). The only difference between **1** and **6** is the orientation of the C-20/21 double bond. Therefore, compound **1** is a geometric isomer of divergolide H (**6**), and **2** is a stereoisomerism of **1.**

The relative configurations of **1** and **2** were established by analysis of 1D and 2D NMR spectroscopic data. The large coupling constants (J > 15.0 Hz) between H-15 and H-16 led to assignment of an *E* configuration of C-15/C-16 double bond. The *Z* configuration of the C-20/21 double bonds was deduced from the relative downfield shift of the allylic methyl group C-20a (δ_C = 20.7 in **1** and **2**) (Table 1), which was further supported by the NOE correlations Me-20a/H-21.

Divergolide Q (**3)** has a molecular formula of $C_{31}H_{41}NO_9$, with 18 *amu* more than that of divergolide A [8] and its congeners E-H.[9] A closer comparison of NMR data (Table 1) with those of divergolides [9] revealed that **3** differs from divergolide F only in the side chain of C-18a and C-18b. The absence of olefinic signals of H-18a and being oxygenated carbon of C-18b indicated that addition reaction of a double bond with water was occurred between C-18a and C-18b (Table 1). The relative configuration o**f 3** is the same with that of **2** by comparison their NMR data and NOE spectrum.

HRESIMS data indicated that divergolides R and S (**4** and **5)** have the same molecular formula of $C_{31}H_{35}NO_8$, and NMR data revealed that they all features a largely conserved divergolide E (**7**) skeleton. Detailed comparing the NMR data (Table 2) of **4** with those of divergolide E,[10] the apparent differences were picked out. The changes of chemical shifts at C-1 (δ_C 73.5 in divergolide E, δ_C 136.7 in **4**), C-22 (δ_C 55.2, δ_H 4.36 in divergolide E and δ_C 126.4 in **4**) indicated that the carbon-carbon double bond was formed between C-1 and C-22 by dehydration. The changes of chemical shift of C-10 (δ_C 124.1 in divergolide E, δ_C 113.5, δ_H 7.55 in **4**) and C-11 (δ_C 211.3 in divergolide E; δ_C 174.9 in **4**) indicated the breakdown of C-10/C-11 bond. Above evidence suggested that **4** was a 10,11-*seco*-1,22-dehydrated divergolide E, namely divergolide S. Compound **5** represents a homologue of **4** but differs in the ester linkage of side chain, the same as the difference between divergolides D and E.[8, 10]

Thus, **5** was determined to be 10,11-*seco*-1,22-dehydrated divergolide D.

Table 1. NMR spectroscopic data for divergolides O-Q (**1** - **3**) and H (**6**) in CD_3COCD_3

	1[a]		**2**[a]		**3**[a]		**6**[a]	
position	δ_C, type	δ_H (*J* in Hz)	δ_C, type	δ_H (*J* in Hz)	δ_C, type	δ_H (*J* in Hz)	δ_C, type	δ_H (*J* in Hz)
1	133.2, C		132.8, C		132.6, C		134.0, C	
2	128.1, C		128.3, C		125.5, C		127.4, C	
3	107.9, CH	7.74, d (2.6)	107.5, CH	7.69, d (2.0)	107.2, CH	7.96, d (2.6)	108.9, CH	7.67, s
4	150.9, C		152.0, C		151.9, C		150.7, C	
5	108.0, CH	6.18, d (2.7)	106.0, CH	6.27, d (1.0)	105.8, CH		108.8, CH	6.24, d (2.2)
6	120.1, C		122.9, C		123.0, C		120.3, C	
7	76.8, CH	5.15, d (5.3)	76.1, CH	5.03, s	76.1, CH	5.03, s	76.8, CH	5.19, d (5.4)
8	49.3, CH	3.21, dd (12.9, 6.5)	52.1, CH	2.60, q (7.2)	52.6, CH	2.57, q (7.2)	49.5, CH	3.19, m
8a	10.0, CH_3	1.03, d (6.8)	15.0, CH_3	1.35, d (7.3)	15.5, CH_3	1.36, d (7.3)	10.1, CH_3	1.01, d (6.8)
9	206.2, C		207.9, C		207.6, C		205.9, C	
10	50.3, CH_2	3.05, d (15.3)	46.5, CH_2	3.10, d (16.8)		2.99, d (16.8)	49.5, CH_2	2.95, d (15.2)
		2.36, d (15.4)		2.22, d (16.9)	49.3, CH_2	2.45, d (16.8)		2.50, d (15.3)
11	105.0, C		103.2, C		102.8, C		104.5, C	
12	39.9, CH_2	1.94, m	40.0, CH_2	1.96, m		2.17, td (13.1, 1.5)	39.9,CH_2	2.16, td (13.7, 4.0)
		1.67, m		1.70, m	39.0, CH_2	1.93 (m)		1.86, m
13	28.1, CH_2	1.70, m,1.51, m	27.9, CH_2	1.72, m, 1.52, m	28.3, CH_2	1.77, (m),c1.20, (m)	27.3,CH_2	1.74, m, 1.41, m
14	46.3, CH	1.91, m	46.4, CH	1.93, m	45.0, CH	1.81 (m)	45.1, CH	1.90, m
14a	29.3, CH_2	1.46, m,1.39, m	29.3, CH_2	1.39, dd (6.4, 7.1)	29.3, CH_2	1.45, (m), 1.38, (m)	29.0, CH_2	1.44, m, 1.35, m
14b	12.2, CH_3	0.90, t (7.4)	12.3, CH_3	0.90, t (7.4)	12.6, CH_3	0.90, t (7.4)	12.2, CH_3	0.88, t (7.4)
15	135.2, CH	5.47,dd (9.0, 15.6)	135.2, CH			5.09, ddd (1.5, 9.3,	136.7, CH	5.49, dd 15.7, 8.3)
				5.48, dd (15.6, 9.3)	136.0, CH	15.8)		
16	133.7, CH	5.71, dd 7.0, 16.0)	133.8, CH	5.72, dd (15.9, 7.4)	125.5, CH	5.63, dd (4.0, 15.4)	131.5, CH	5.59, dd (15.7, 6.9)
17	75.1, CH	4.24, m	75.1, CH	4.25, d (6.1)	78.5, CH	5.17, (m)	74.1, CH	4.29, dd (6.7, 3.0)
18	76.9, CH	5.66, dd (5.6,13.3)	77.1, CH	5.67, dd (2.0, 9.7)	71.0, CH	4.17, (m)	74.5, CH	5.66, dd (9.4, 3.3)
18a	122.2, CH	5.52, dt (1.2, 9.2)	122.1, CH	5.52, dt (1.2, 9.2)	44.4, CH_2	1.72, (m)	121.1, CH	5.37, d (9.3)
18b	26.1, CH_3	1.74, d (0.8)	26.1, CH_3	1.74, d (0.9)	28.7, CH_3	1.29, s	26.4, CH_3	1.76, d (0.5)
18c	137.9, C		137.9, C		70.9, C		139.3, C	
18d	18.8, CH_3	1.78, d (0.9)	18.8, CH_3	1.79, d (0.9)	31.8, CH_3	1.24, s	18.9, CH_3	1.79, s
19	167.7, C		167.8, C		168.6, C		166.84, C	
20	133.1, C		133.1, C		131.3, C		133.8, C	
20a	20.7, CH_3	2.10, s	20.7, CH_3	2.08, brs	20.6, CH_3	2.05, s	13.1, CH_3	1.94, s
21	135.6, CH	6.27, ddd (1.3, 7.2, 9.9)	135.7, CH	6.26, ddd, (10.1, 7.4, 1.3)	137.6, CH	6.29, dd (7.1, 10.7)	133.1, CH	6.95, d (6.0)
22	41.0, CH_2	3.87, dd (10.1, 14.2)	40.5, CH_2	3.88, dd (13.8, 10.3)		4.19, m	38.5, CH_2	3.44, m
		2.97, dd (7.1, 14.2)		2.92, dd （13.9, 7.1)	41.0, CH_2	2.82, dd (11.4, 7.2)		3.21, m
23	167.7, C		167.8, C		168.5, C		166.8, C	
NH		8.56, s		8.68, s		8.89, s		7.99, s

Table 2. NMR spectroscopic data for divergolides R and S (**4** and **5**) and divergolide E (**7**) in CD_3COCD_3

position	**4**		**5**		**7**	
	δ_C, type	δ_H (*J* in Hz)	δ_C, type	δ_H (*J* in Hz)	δ_C, type	δ_H (*J* in Hz)
CH	136.7, C		136.7, C		73.2, C	
2	152.5, C		152.5, C		160.0, C	
3	105.7, CH	5.92, s	105.7, CH	5.93, s	103.1, CH	5.81, s
4	184.2, C		184.2, C		183.9, C	
5	131.2, C		131.7, C		130.5, C	
6	122.5, C		122.5, C		133.8, C	
7	131.4, CH	7.51, s	131.2, CH	7.52, s	133.4, CH	7.67, s
8	130.8, C		130.8, C		132.1, C	
8a	16.6, CH_3	2.26, s	16.6, CH_3	2.26, s	16.7, CH3	2.31, s
9	158.8, C		158.8, C		153.4, C	
10	113.5, CH	7.55, s	113.5, CH	7.56, s	130.9,C	
11	174.9, C		174.9, C		211.5,C	
12	32.1, CH_2	2.28, 2.21, m	32.1, CH_2	2.31, 2.23, m	42.6, CH_2	α: 2.42, ddd (2.7, 5.5, 13.1) β: 2.62, dt (2.3, 13.1)
13	30.8, CH_2	1.74, m 1.44, m	30.6, CH_2	1.72, 1.50, m	35.3, CH_2	1.33, m
14	44.9, CH	1.94, m	45.2, CH	1.95 (m)	43.8, CH	1.42 (q, 10.6/9.4)
14a	28.8, CH_2	1.42, m 1.29, m	28.7, CH_2	1.44 , 1.29, m	30.6, CH_2	1.29, m; 1.03, m
14b	12.1, CH_3	0.88, t (7.4)	12.1, CH_3	0.87, t (7.4)	12.5, CH_3	0.70, t (6.7)
15	137.1, CH	5.51, dd (8.3, 15.4)	127.5, CH	5.53, d (7.4,A2 spin system)	133.4, CH	5.11, ddd (1.6, 9.7, 15.4)
16	131.6, CH	5.56, dd (6.0, 15.4)	139.9, CH	5.54, d (5.0, A_2 spin system)	130.5, CH	3.95, d (15.5)
17	74.6, CH	4.32, t (6.7)	80.1, CH	5.34, m	73.2, CH	4.16, br s
18	76.1, CH	5.65, dd (7.0, 9.5)	70.2, CH	4.59, dd (7.4, 9.0)	76.1, CH	5.44, dd (3.2. 9.6)
18a	121.9, CH	5.33, dt (1.2, 9.5)	125.4, CH	5.27, dt (1.2, 9.0)	120.1, CH	4.73, d (9.5)
18b	19.0, CH_3	1.84, d (1.0)	18.7, CH_3	1.73,d (0.9)	139.7, C	
18c	139.6, C		136.7, C		26.3, CH_3	1.61, s
18d	26.1, CH_3	1.78, d (0.9)	26.0, CH_3	1.74, d (0.9)	18.7, CH_3	1.72, s
19	166.9, C		166.8, C		167.5, C	
20	137.0, C		136.5, C		137.2, C	
20a	16.2, CH_3	1.94, d (1.2)	16.2, CH_3	1.95, d (1.2)	21.5, CH_3	2.16, d (1.3)
21	128.9, CH	7.56, d (1.0)	129.0, CH	7.59, d (1.0)	127.5, CH	6.44, dd (0.7, 10.8)
22	126.4, C		137.1, C		55.3, CH	4.36, d (10.8)
23	169.7, C		169.7, C		175.1, C	

The large coupling constants (J > 15.0 Hz) between H-15 and H-16 led to assignment of an *E* configuration of C-15/C-16 double bond in **4** and **5**. Interestingly, strong NOE correlations were observed between H-20a and H-15/H-16, and H-14a and H-15/H-16 in **4**, suggesting that the C-18/O-18 bond can rotate freely and thus further supporting the breakage of C-10/C-11 bond to form *seco* variant (**4**, **5**).

Divergolides O-S were tested for their cytotoxicities against human tumor MDA-MB-231, PC3 and HeLa cell lines. All of them were found to be weak or no cytotoxic activities. Whereas, divergolide E (**7**) displayed remarkable activities against MDA-MB-231, PC3 and HeLa with IC_{50} of 2.6, 1.5, and 0.6 μM, respectively. Divergolides were reported to show weak to moderate activity against Gram-positive bacteria, such as divergolide A and I [8, 11] against *Mycobacterium vaccae*; whereas only divergolide D showed cytotoxic activities against several cell lines with IC_{50} values ranging from 1.0 to 2.0 μM, [8] which suggested that the ansamycin bridge ring was important for the biological activity.

Ansamycins, such as rifamycins[12-14], kanglemycin[15] and naphthomycin[16, 17], are reported as famous antibacterial agents. *Salmonella enterica* is an important pathogen of humans and animals. And it has type III secretion system (T3SS) as its major virulence factor. The pathogenicity of *S. enterica* mainly depends on two T3SSs, encoded by Salmonella pathogenicity island 1 (SPI-1) and SPI-2. SPI-1 mediates invasion of the intestinal epithelium and induction of proinflammatory responses through injecting effector proteins into host cells, while SPI-2 regulates the replication of bacteria in host phagocytic cells. [18] To exploit novel antibacterial agents targeting SPI-1, the effect of compounds **1** – **6** on secretion of SPI-1 (Salmonella Pathogenicity Island-1) effector proteins was also assessed *in vitro*[19]. Type three T3SS is an injector-like secretion apparatus in many gram-negative bacteria. It could transport effector proteins from bacterial cytoplasm into eukaryotic host cells to facilitate the invasion and dissemination of pathogens.[20] T3SS has been becoming an attractive drug target for developing novel antivirulence agents, because it is highly conserved among different gram-negative bacteria,[21, 22] and not essential for bacterial growth.[23, 24] The results indicated that **4** and **5** significantly inhibited the secretion of SPI-1 effectors, SipA/B/C/D, but no effect on FliC, and **1**, **2**, **3** and **6** showed weaker or no inhibitory effect on SPI-1 in the concentration of 100 μM, respectively (Fig.2A). Compound **4**

showed obviously concentration gradient inhibition, even in the concentration of 50 μM (Fig.2B). Whereas, **5** represented no significant concentration gradient inhibition. In the light of the weak cytotoxicity, the mechanism of action of **4** and **5** on T3SS might well repay investigation.

Ansamycins are characterized by an aromatic nucleus connected with a polyketide chain back to a nonadjacent position through an amide bond.[25, 26] Both divergolides [8] and hygrocins [27, 28] belong to nonaketide with highly diversified structures resulted from diverse post-PKS modifications. The *seco* divergolides M and N from *S.* sp. HKI0576 [11] obviously represent pathway intermediates that were prematurely released from the modular assembly line. *Seco* divergolide L maybe formed by decarboxylation after spontaneous hydrolysis of the macrolide.[11] It happens that there is a similar case, *seco* variants congeners (**4** and **5**) are similar to hygrocins I and J (Fig. S2) isolated from *Streptomyces* sp. SR101OE*hgc1* and their biosynthetic pathway have been proposed from a spontaneous reversed-Claisen reaction.[29]

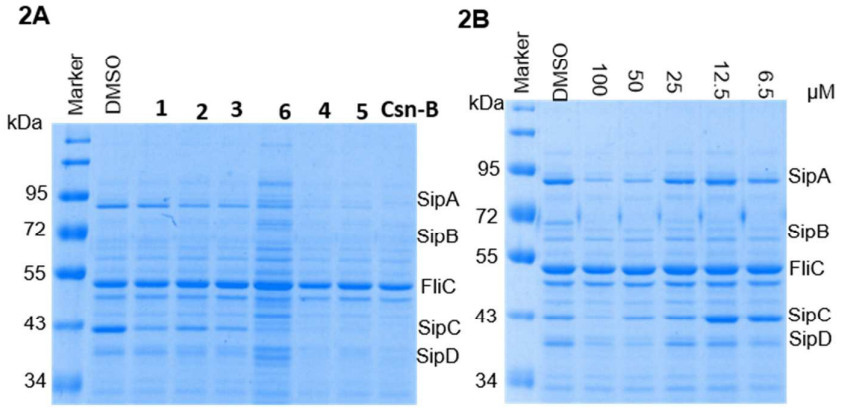

Fig.2A Divergolides O–S (**1**–**5**) and H (**6**) inhibited the secretion of *Salmonella enterica* serovar Typhimurium invasion-associated SPI-1 effector proteins *in vitro*. (SipA/B/C/D, SPI-1 effector proteins; FliC, flagellar filament protein; DMSO as control) *Salmonella enterica* serovar Typhimurium UK-1*χ*8956 (ΔP *rpoS*183::TT *ara*C PBAD *rpo*S) was grown in LB medium supplemented with 0.2% L-arabinose in the presence of solvent control or tested compounds at a final concentration of 100 μM, respectively. The effector proteins of SPI-1 in the supernatant of culture were precipitated by 10% TCA and analyzed by 10% SDS-PAGE followed by staining with Coomassie Blue. SipA/B/C/D, SPI-1 effector proteins; FliC, flagellin of *Salmonella*.

Fig.2B Divergolides R (**4**) inhibited the secretion of SPI-1 effectors in a dose-dependent manner (at a range of concentrations from 50 to 100 μM) and did not affect growth of *S. enterica* serovar Typhimurium.

Experimental section

General experimental procedures. The optical rotation was measured using an Anton Paar MCP200 polarimeter. The IR spectrum was recorded on a Thermo Nicolet NEXUS 470 FT-IR spectrometer in KBr discs. NMR spectra were recorded on a Bruker Avance DRX-600 spectrometer operating at 600 (^{1}H) and 150 (^{13}C) MHz. HRESIMS was carried out on an LTQ-Orbitrap XL. High-performance liquid chromatography (HPLC) were performed on an Agilent 1260 instrument; ZORBAX Eclipse XDB-C_{18} (9.4 × 250 mm). All solvents were analytical grade. Silica gel (200−300 mesh; Qingdao Haiyang Chemical Company Ltd., Qingdao, China) and Sephadex LH-20 (25−100 μm; Pharmacia Biotek, Denmark) were used for column chromatography. Thin-layer chromatography (TLC) was carried out with glass percolated silica gel GF_{254} plates (Qingdao Haiyang Chemical Company Ltd.). Compounds were visualized under UV light and by spraying with H_2SO_4/EtOH (1:9, v/v), followed by heating.

Strain and fermentation. Strain W112OE*div8* was constructed by our previously work.[6, 10] The strain was cultured in Petri dishes with *ca*. 20 mL ISP3 medium (1.5% agar, 2% oatmeal, 0.1% trace element solution, pH 7.2) with a total volume of 40 litres for 14 d at 28°C.

Extraction and isolation.

The culture (40 L) was extracted three times with EtOAc–MeOH (80 : 15, *v/v)* to obtain the extract. The crude extract was partitioned between petroleum ether and 95% MeOH to afford MeOH extract.

The MeOH extract (12.8 g) was chromatographed over MPLC (120 g RP-18 silica gel; 30%, 50%, 70%, 80%, 100%MeOH, 2 L each, respectively) to obtain Fr. 1-18. Fr. 10 was combined with Fr. 11 in accordance with the results of TLC. The combined Fr. 11 (1.6836 g) was purified by *Sephadex* LH-20 (120 g) eluted with MeOH to give Fr. 11a-f. Fr. 11d (784.7 mg) was further chromatographed over MPLC (60 g, RP-18; 50%, 60%, 70%, 100% MeOH, 300 mL each, respectively) to obtain Fr. 11d1-d4. Fr. 11d2 (335.4 mg) was further purified by MPLC repeated two times and finally purified by HPLC (50% CH_3CN, 4.0 mL/min) to obtain **7** (t_R 8 min, 10 mg). Fr. 11d3 (66.8 mg) was further purified by *Sephadex* LH-20 (120 g) eluted with

MeOH, then the main part was subjected to RP-18 CC (MeOH/H_2O as gradient) and **6** (t_R 16.5 min, 4 mg) was finally obtained by *Sephadex* LH-20 (60 g, acetone) and HPLC (45% CH_3CN, 4.0 mL/min). Fr. 11d4 (160 mg) was further purified by MPLC and *Sephadex* LH-20 (60 g) and finally purified by HPLC (45% CH_3CN, 4.0 mL/min) to obtain **3** (t_R 14 min, 5 mg). Fr.11d4 was further purified by *Sephadex* LH-20 (60 g) eluted with acetone, and further purified by HPLC (55% CH_3CN, 4.0 mL/min) to yield **1** (t_R 10 min, 5 mg) and **2** (t_R 10.5 min, 6 mg).

Fr. 12 (1.1883 g) was chromatographed over MPLC (100 g, RP-18; 50%, 60%, 65%, 70%, 100% MeOH, 300 mL each, respectively) to obtain Fr. 12.1-6. Fr. 12.4 (367.7 mg) was further purified by *Sephadex* LH-20 (60 g, acetone), and purified by HPLC (50% CH_3CN, 4.0 mL/min) to yield **4** (t_R 5.8 min, 5 mg) and **5** (t_R 7.0 min, 6 mg)

.

Divergolide O (**1**): light yellow powder; $[\alpha]_D^{20}$ = +244.2 (*c* 0.050, MeOH); UV/Vis: λ_{max} nm (log ε): 310.0 (3.31), 245.0 (4.26), 220.0 (4.14); ^1H and ^{13}C NMR data, see Table 1; ESIMS: *m/z* 554.5 $[M + H]^+$, 576.5 $[M + Na]^+$; HRESIMS: *m/z* 554.2748 $[M + H]^+$ (calcd. for $C_{31}H_{39}NO_8^+$, 554.2676).

Divergolide P (**2**): yellow powder; $[\alpha]_D^{20}$ = +34.24 (*c* 0.011, MeOH); UV/Vis: λmax nm (log ε): 310.0 (3.31), 245.0 (4.26), 220.0 (4.14); ^1H and ^{13}C NMR data, see Table 1; ESIMS: *m/z* 554.5 $[M + H]^+$, 576.5 $[M + Na]^+$, 571.6 $[M + NH_4]^+$; HRESIMS: *m/z* 554.2749 $[M + H]^+$ (calcd. for $C_{31}H_{39}NO_8^+$, 554.2748)..

Divergolide Q (**3**): light yellow powder; $[\alpha]_D^{20}$ = -18.79 (*c* 0.033, MeOH); UV/Vis: λmax nm (log ε): 310.0 (3.31), 245.0 (4.26), 220.0 (4.14); ^1H and ^{13}C NMR data, see Table 1; ESIMS: *m/z* 572.4 $[M + H]^+$, 594.5 [M + Na]+, 589.5 $[M + NH_4]^+$, HRESIMS: *m/z* 572.2855 $[M + H]^+$ (calcd. for $C_{31}H_{41}NO_9^+$ 572.2854).

Divergolide R (**4**): red powder; $[\alpha]_D^{20}$ = -14.7 (*c* 0.423, MeOH); IR (KBr) V_{max} 3389, 2964, 2926, 1715, 1654 cm^{-1};. ^1H and ^{13}C NMR data, see Table 2; HRESIMS: *m/z* 550.2433 $[M + H]^+$ (Calcd. for $C_{31}H_{36}NO_8^+$, 550.2435).

Divergolide S (**5**): red powder; $[\alpha]_D^{20}$ = -29.8 (*c* 0.235, MeOH); IR (KBr) V_{max} 3412, 2963, 2926, 1715, 1653 cm^{-1}; ^1H and ^{13}C NMR data, see Table 2; HRESIMS: *m/z* 550.2435 $[M + H]^+$ (Calcd. for $C_{31}H_{36}NO_8^+$, 550.2435).

Cytotoxicity Test

The *in vitro* antiproliferative activities were assessed with a sulforhodamine B (SRB) assay[30].

Effect of compounds 1–6 on the secretion of SPI-1 effector proteins. *Salmonella enterica* serovar Typhimurium UK-1 χ8956 (ΔP rpoS183: TT araC PBAD rpoS) was used in this study [31], which was cultivated in LB broth (1% tryptone, 0.5% yeast extract, 1% NaCl, pH 7.4) or on LB agar plates with 0.2% L-arabinose at 37ºC or 25ºC. The assay of isolation and detection of effector proteins of SPI-1 (Salmonella Pathogenicity Island-1) were performed as previously described[19]. Changing the temperature of bacterial culture was used to induce SPI-1 to promote the secretion of effector proteins. In short, bacterial culture was incubated overnight at 25ºC with agitation. Compounds **1**–**6** at 100 *μ*M or solvent control were added into the diluted cultures of 10 times the next day and the cultures were continued to grow at for 4 h 37ºC with agitation. Cytosporone B (CsnB) was chosen as a positive control[19]. The secreted proteins in the supernatant of culture were precipitated by 10% trichloroacetic acid (TCA). Sediments were dissolved in 1× sample buffer and heated for 10 min at 95ºC to denature the proteins. The protein samples were detected by SDS-PAGE followed staining with Coomassie Blue.

Acknowledgements

This work was supported in part by the National Natural Science Foundation of China (81373304, 81530091), and the Independent Innovation Foundation of Shandong University (IIFSDU, 2014JC027) and Program for Changjiang Scholars and Innovative Research Team in University (IRT13028).

Notes and references

1. C. DeBoer, P. A. Meulman, R. J. Wnuk and D. H. Peterson, *J Antibiot.*, 1970, **23**, 442-447.
2. J. M. Cassady, K. K. Chan, H. G. Floss and E. Leistner, *Chem Pharm Bull (Tokyo)*, 2004, **52**, 1-26.
3. E. Higashide, M. Asai, K. Ootsu, S. Tanida, Y. Kozai, T. Hasegawa, T. Kishi, Y. Sugino and M. Yoneda, *Nature*, 1977, **270**, 721-722.
4. J. E. Thiemann, C. Hengeller and A. Virgilio, *Nature*, 1962, **193**, 1104-1105.
5. Q. Kang, Y. Shen and L. Bai, *Nat Prod Rep*, 2012, **29**, 243-263.
6. H. X. Wang, Y. Y. Chen, L. Ge, T. T. Fang, J. Meng, Z. Liu, X. Y. Fang, S. Ni, C. Lin, Y. Y. Wu, M. L. Wang, N. N. Shi, H. G. He, K. Hong and Y. M. Shen, *J Appl Microbiol,* 2013, **115**, 77-85.
7. Y. Wu, C. Lu, X. Qian, Y. Huang and Y. Shen, *Curr Microbiol*, 2009, **59**, 475-482.

8. L. Ding, A. Maier, H. H. Fiebig, H. Gorls, W. H. Lin, G. Peschel and C. Hertweck, *Angew Chem Int Ed Engl*, 2011, **50**, 1630-1634.
9. Z. Xu, M. Baunach, L. Ding, H. Peng, J. Franke and C. Hertweck, *Chembiochem*, 2014, **15**, 1274-1279.
10. S. R. Li, G. S. Zhao, M. W. Sun, H. G. He, H. X. Wang, Y. Y. Li, C. H. Lu and Y. M. Shen, *Gene*, 2014, **544**, 93-99.
11. L. Ding, J. Franke and C. Hertweck, *Org Biomol Chem*, 2015, **13**, 1618-1623.
12. S. Fueresz and M. T. Timbal, *Chemotherapy*, 1963, **257**, 200-208.
13. A. Sanfilippo, C. Della Bruna, L. Marsili, E. Morvillo, C. R. Pasqualucci, G. Schioppacassi and D. Ungheri, *J. Atibiot*, 1980, **33**, 1193-1198.
14. C. K. Murphy, E. Karginova, D. Sahm and D. M. Rothstein, *J Antibiot*, 2007, **60**, 572-576.
15. N. J. Wang, Y. Fu, G. H. Yan, G. H. Bao, C. F. Xu and C. H. He, *J Antibiot*,, 1988, **41**, 264-267.
16. T. H. Williams, *J Antibiot*, 1975, **28**, 85-86.
17. T. Mukhopadhyay, C. M. Franco, G. C. Reddy, B. N. Ganguli and H. W. Fehlhaber, *J Antibiot*, 1985, **38**, 948-951.
18. M. Hensel, *International journal of medical microbiology : IJMM*, 2004, **294**, 95-102.
19. J. Li, C. Lv, W. Sun, Z. Li, X. Han, Y. Li and Y. Shen, *Antimicrob Agents Chemother*, 2013, **57**, 2191-2198.
20. D. Aiello, J. D. Williams, H. Majgier-Baranowska, I. Patel, N. P. Peet, J. Huang, S. Lory, T. L. Bowlin and D. T. Moir, *Antimicrob Agents Chemother*, 2010, **54**, 1988-1999.
21. L. M. Stamm and M. B. Goldberg, *VIP*, 2011, **331**, 1147-1148.
22. L. J. Worrall, E. Lameignere and N. C. Strynadka, *Curr Opin Microbiol*, 2011, **14**, 3-8.
23. R. Nordfelth, A. M. Kauppi, H. A. Norberg, H. Wolf-Watz and M. Elofsson, *Infect Immun*, 2005, **73**, 3104-3114.
24. E. Crabill, A. Joe, A. Block, J. M. van Rooyen and J. R. Alfano, *Plant Physiology*, 2010, **154**, 233-244.
25. W. Wehrli, *Top Curr Chem*, 1977, **72**, 21-49.
26. H. G. Floss, *J Nat Prod*, 2006, **69**, 158-169.
27. C. Lu, Y. Li, J. Deng, S. Li, Y. Shen and H. Wang, *J Nat Prod*, 2013, **76**, 2175-2179.
28. P. Cai, F. Kong, M. E. Ruppen, G. Glasier and G. T. Carter, *J Nat Prod*, 2005, **68**, 1736-1742.
29. S. R. Li, C. H. Lu, J. H. Ou, J. J. Deng and Y. M. Shen, *RSC Advance*, 2015, **5**, 83843-83846.
30. V. Vichai and K. Kirtikara, *Nature protocols*, 2006, **1**, 1112-1116.
31. R. Curtiss, 3rd, S. Y. Wanda, B. M. Gunn, X. Zhang, S. A. Tinge, V. Ananthnarayan, H. Mo, S. Wang and W. Kong, *Infect Immun*, 2009, **77**, 1071-1082.